Nuclear effects in $g_{1A}(x,Q^2)$ at small x in deep inelastic scattering on ^{7}Li and ^{3}He

V. Guzey
Department of Physics, The Pennsylvania State University, University Park, Pennsylvania 16802

M. Strikman*
Department of Physics, The Pennsylvania State University, University Park, Pennsylvania 16802
and Deutsches Elektronen-Synchrotron (DESY), Hamburg, Germany
(Received 30 March 1999; published 16 December 1999)

We suggest using polarized nuclear targets of ^{7}Li and ^{3}He to study nuclear effects in the spin-dependent structure functions $g_{1A}(x,Q^2)$. These effects are expected to be enhanced by a factor of 2 as compared to the unpolarized targets. We predict a significant x dependence at 10^{-4}–$10^{-3} \leqslant x \leqslant 0.2$ of $g_{1A}(x,Q^2)/g_{1N}(x,Q^2)$ due to nuclear shadowing and nuclear enhancement. The effect of nuclear shadowing at $x \approx 10^{-3}$ is of an order of 16% for $g^{n.s.\ 3/2}_{1A=7}(x,Q^2)/g^{n.s.}_{1N}(x,Q^2)$ and 10% for $g^{n.s}_{1A=3}(x,Q^2)/g^{n.s.}_{1N}(x,Q^2)$. By imposing the requirement that the Bjorken sum rule is satisfied we model the effect of enhancement. We find the effect of enhancement at $x \approx 0.125$ (0.15) to be of an order of 20 (55)% for $g^{n.s.\ 3/2}_{1A=7}(x,Q^2)/g^{n.s.}_{1N}(x,Q^2)$ and 14 (40)% for $g^{n.s}_{1A=3}(x,Q^2)/g^{n.s.}_{1N}(x,Q^2)$, if enhancement occupies the region $0.05 \leqslant x \leqslant 0.2$ $(0.1 \leqslant x \leqslant 0.2)$. We predict a 2% effect in the difference of the scattering cross sections of deep inelastic scattering of an unpolarized projectile off ^{7}Li with $M_J = 3/2$ and $M_J = 1/2$. We also show explicitly that the many-nucleon description of deep inelastic scattering off ^{7}Li becomes invalid in the enhancement region $0.05 < x \leqslant 0.2$.

PACS number(s): 25.10.+s, 24.70.+s, 25.30.−c, 24.85.+p

I. INTRODUCTION

It is now well known that nuclear effects are important in deep inelastic scattering (DIS) of leptons on nuclear targets. For example, if we consider the ratio of structure functions $R_A(x,Q) = (F_{2A}(x,Q)/A)/(F_{2D}(x,Q)/2)$ as a function of x, we can distinguish various regions over the range of x from 10^{-5}–10^{-4} to $x = 1$ and beyond, where different nuclear mechanisms govern the particular behavior of $R_A(x,Q)$. In this paper we will consider only the region $x \leqslant 0.2$.

For $x < 0.05$ $R_A(x,Q)$ is smaller than 1 due to nuclear shadowing. It arises from coherent interactions of the incoming virtual photon with several nucleons of the target nucleus in the target rest frame. These interactions occur over the distance $l_c = t_f \sim 1/(2m_N x)$, see Eq. (1). When $l_c \sim r_{NN} = 1.7$ fm, the average internucleon distance in nuclei, the coherence effects become suppressed. This sets the upper limit to the region of nuclear shadowing at $x \approx 0.05$. In the infinite momentum frame the leading twist shadowing can be viewed as a depletion of the nuclear parton densities due to a spatial overlap of partons belonging to different nucleons. Nuclear shadowing phenomena for the structure function $F_{2A}(x,Q^2)$ and for the nuclear gluon parton density $G_A(x,Q^2)$ have been discussed in the literature for a long time. Current data on shadowing for $F_{2A}(x,Q^2)$ are consistent with the Gribov theory [1] which relates this phenomenon to diffraction on protons, for the recent discussion and references see [2].

For $x > 0.05$ up to 0.2–0.25 $R_A(x,Q^2)$ first grows and becomes larger than 1, then decreases and approaches 1 from above. The dynamical mechanism of enhancement has not been understood yet. It is present for the gluon and valence quark parton densities [3–5] and it is absent for the sea quarks [6].

Thus, nuclear shadowing and enhancement are the two phenomena that modify the structure functions of nuclei at 10^{-5}–$10^{-4} \leqslant x \leqslant 0.2$–$0.25$ and produce their nontrivial x dependence. In spite of the potential importance of the nuclear shadowing and enhancement effects until recently they were ignored in the studies of nuclear effects in polarized nuclear structure functions [7] and their applications to the Bjorken sum rule for nuclei [8].

The study of nuclear shadowing provides unique information about the space-time picture of strong interactions and, in particular, about the interplay of soft and hard effects. The uncertainties due to the wave functions of nuclei are small since the large internucleon distances give the dominant contribution.

Another application of studies on nuclear shadowing effects at low x is related to the neutron spin-dependent structure function. As it was pointed out in our original paper [9], when one extracts the neutron spin-dependent structure function $g_{1n}(x,Q^2)$ from the ^{3}He data, shadowing and enhancement should be taken into consideration. If it is not done, this might lead to a misinterpretation of the data.

We propose to study experimentally effects of nuclear shadowing and enhancement using polarized nuclei of ^{7}Li and ^{3}He because for these nuclei nuclear shadowing and enhancement are larger by a factor of 2 as compared to the unpolarized targets [9].[1]

*On leave of absence from The Pennsylvania State University.

[1]A similar enhancement is present for deuteron targets, though it is very difficult to observe it experimentally since $g_{1d}(x,Q^2) \ll g_{1p}(x,Q^2)$ for small x. For an extensive discussion of scattering off polarized deuteron targets see [10].

Basically, this is because in the case of unpolarized scattering due to N identical exchanges a factor $1/N!$ is present in the Glauber series, while in the case of polarized scattering the exchange generating $g_{1A}(x,Q^2)$ is not identical to the rest of the exchanges, leading to a factor $1/(N-1)!$. Hence, for the case of light nuclei where triple rescatterings can be neglected the shadowing effect is enhanced by a factor of 2. Also it is instructive to consider the limit of large atomic number A. In this case scattering off a polarized valence nucleon can contribute to $g_{1A}(x,Q^2)$ only if the nucleon is near the edge since for the central impact parameters the interaction would be black and, hence, would not contribute to the spin asymmetry. As a result in this limit one would get for small enough x that $g_{1A}(x,Q^2) \propto A^{-2/3} g_{1N}(x,Q^2)$.

Polarized ^{3}He has been used extensively over years. It seems feasible to reach large values of polarization for a ^{7}Li target as well [11].

In the present paper we calculated nuclear shadowing of the spin-dependent structure functions $g_{1A}^{n.s.\ 3/2}(x,Q^2)$ and $g_{1A}^{n.s.\ 1/2}(x,Q^2)$ using an extension of the Gribov theory of nuclear shadowing in DIS [1].

Obviously this changes the contribution to the Bjorken sum rule at small x. Hence this depletion should be compensated by some enhancement such that these two effects do not alter the ratio of the integrated nuclear to nucleon nonsinglet spin-dependent structure functions R, which is determined by the Bjorken sum rule. We used this as a guiding principle to model the effect of enhancement for the region $0.05\ (0.1) \leqslant x \leqslant 0.2$, where enhancement is the dominant nuclear effect.

II. NUCLEAR EFFECTS AT SMALL x IN $g_{1A}(x,Q^2)$ FOR ^{7}Li

As we pointed out in the Introduction the fact that it is possible to create targets of polarized ^{7}Li makes this nucleus a useful tool for studying spin-dependent structure functions. According to the shell model, nuclear polarization will be predominantly (87%) due to a single proton [12]. This will enhance shadowing and enhancement effects for the polarized target as compared to the unpolarized one by a factor of 2. An advantage of using ^{7}Li as compared to ^{3}He, i.e., a nucleus with the ''valence'' (in the sense of the shell model) proton rather than neutron, is that the proton spin-dependent structure function $g_{1p}(x,Q^2)$ is known with a better accuracy than the neutron spin-dependent structure function $g_{1n}(x,Q^2)$. This matters because one can see from the structure of our answer that we compute the ratio of nuclear to nucleon spin-dependent structure functions. Thus, in order to find the nuclear structure function alone, we need to know the nucleon structure function with the best accuracy as possible.

It was realized a long time ago that if the transition time of a photon with a four-momentum Q into a quark-gluon configuration with mass M_{h_i} is larger than the typical interaction time, which is of the size of the target, i.e., when

$$t_f = \frac{2\nu}{Q^2 + M_{h_i}^2} \approx \frac{1}{2m_N x} > 2R_A, \tag{1}$$

then the incoming virtual photon (could be a real one as well) reveals its hadronic properties. For example, DIS on nuclei displays shadowing, i.e., the effect when the nuclear structure function per nucleon is smaller than the nucleon structure function. Throughout this paper we will refer to these quark-gluon configurations as states $|h_i\rangle$.

If Eq. (1) is satisfied, then the total photoabsorption cross section of photons on a nuclear target with the atomic number A can be presented as

$$\sigma_{\gamma^* A}(Q^2) = \sum_{h_i} |\langle \gamma^* | h_i \rangle|^2 \sigma_{h_i A}. \tag{2}$$

Note that since Eq. (2) is an effective one, we can think of states $|h_i\rangle$ as eigenstates of the scattering matrix, i.e., no nondiagonal transitions need to be introduced.

To elaborate more on the cross sections $\sigma_{h_i N}$ and $\sigma_{h_i A}$ and their relevance to our problem it is instructive to go to the infinite momentum frame of the target. The spin-dependent structure function $g_1(x,Q^2)$ can be written as a convolution with quark nonsinglet Δq_{ns}, singlet Δq_s, and gluon ΔG polarized parton densities [13]

$$g_1(x,Q^2) = \frac{\langle e^2 \rangle}{2} (C_{ns} \otimes \Delta q_{ns} + C_S \otimes \Delta q_s + 2n_f C_g \otimes \Delta G), \tag{3}$$

where $\langle e^2 \rangle = n_f^{-1} \Sigma_{i=1}^{n_f} e_i^2$, $\otimes$ denotes convolution with respect to x. Therefore, nuclear shadowing of $g_{1A}(x,Q^2)$ at small x is due to nuclear shadowing of the spin-dependent structure functions. The recent analysis of the diffractive data of HERA [2] showed that in unpolarized deep inelastic scattering on nuclei the nuclear shadowing for gluon parton densities should be larger by a factor of 3 than that for the quark parton densities. Namely, at $x \approx 10^{-3}$ and Q is of an order of few GeV, the effective cross section of interaction of $|h_i\rangle$ with the nucleon in the quark channel $\sigma_{\rm eff} = 17$ mb, and in the gluon channel $\sigma_{\rm eff} = 50$ mb. The notion of the quark channel is referred to the γ^* interaction with the quark field of the target and the gluon channel is referred to the interaction with the gluon field of the target.

Hence, we make *a natural hypothesis* that the strengths of interactions in the sea quark channel of the unpolarized DIS and polarized channels are similar. Since the shadowing in the quark channel is characterized by a relatively small average interaction strength, it is a good approximation to replace the sum over hadronic components of the photon by a single term with the typical mass $M_h = Q$ and the cross sec-

tion $\sigma_{hN}=\sigma_{\rm eff}=17$ mb. This choice corresponds to the analysis of shadowing for nuclei with $A\geqslant 12$ in color screening models, where the fit to the experimental data at $x\sim 10^{-3}$–10^{-2}, $Q^2\sim 2$–5 GeV^2 required $\sigma_{\rm eff}=\langle\sigma^2\rangle/\langle\sigma\rangle=17$ mb (see [9] and references therein). Here the averaging occurs with the measure of the probability of the corresponding configurations $|h_i\rangle$ in the photon wave function. The HERA diffractive ep data lead to a similar value of $\sigma_{\rm eff}\approx 14\pm 3.5$ mb at somewhat smaller x and larger Q^2.

A recent global next-to-leading order QCD analysis [13] of the world data from CERN, SLAC, and DESY has showed that the present accuracy of the data is not sufficient to make any qualitative conclusions about the magnitude of the polarization of gluons $\Delta G(x,Q^2)$. Hence, we will disregard the contribution of $\Delta G_A(x,Q^2)$ to $g_{1A}(x,Q^2)$ in this paper. At the same time we will estimate the amount of nuclear shadowing in $\Delta G_A(x,Q^2)$ for ^{3}He which turns out to be large and may be possible to investigate at HERA in the polarized eN mode.

In the discussed approximation the problem of deep inelastic scattering of a virtual photon is reduced to scattering of an effective hadronic (quark-gluon) state. The latter can be treated using the Gribov-Glauber formalism.

Note that due to cross section fluctuations in the incoming photon the triple scattering term should contain $\langle\sigma^3\rangle$, where one averages over fluctuations of the size of the projectile. Our assumption that the incoming photon interacts with the target through the effective state $|h\rangle$ means that we have replaced $\langle\sigma^3\rangle$ by $(\langle\sigma^2\rangle)^2/\langle\sigma\rangle=\sigma_{\rm eff}^2\langle\sigma\rangle$. Since the triple term is numerically small this substitution is of high accuracy.

Note that differently from the hadron-nucleus scattering, one has to take into account a nonvanishing longitudinal momentum $q_\parallel$ transferred to the target in the transition $\gamma\rightarrow|h\rangle$, $q_\parallel=(Q^2+M_h^2)/2\nu\approx 2m_N x$, see, e.g., [14].

In our calculation we used the ground-state wave function of ^{7}Li given by the nuclear shell model [12]. This is certainly an oversimplified model for the ^{7}Li wave function. However, the shadowing effects are mostly determined by the long-range part of the wave function and should not be sensitive to the refinements of the wave function.

The impulse approximation is certainly more sensitive to the degree of the nucleon polarization in the nucleus than to the effects of the Fermi motion, which are small for $x\geqslant 0.5$. So, in the kinematics that we discuss one can write in the impulse approximation [7]

$$g_{1A}(x,Q^2)=P_p g_{1p}(x,Q^2)+P_n g_{1n}(x,Q^2), \tag{4}$$

where P_p (P_n) is polarization of the proton (the neutron) in ^{7}Li.

We find that the modification of $g_{1A}(x,Q^2)$ due to the nuclear shadowing cannot be mimicked by any reasonable variation of P_p and P_n, see discussion in Sec. III.

In most of our analyses of this section the z component of the total angular momentum of ^{7}Li, M_J, is chosen to be 3/2 or $-3/2$. The axis of quantization is along the virtual photon direction. Therefore, target polarization discussed in our paper is always longitudinal. We will show that when the target is longitudinally polarized with $M_J=1/2$ the discussed effects are suppressed. For the components of the wave function of ^{7}Li with $M_J=3/2$, 1/2, $-1/2$, $-3/2$ see Appendix A.

The valence part of the total wave function of ^{7}Li consists of two valence neutrons and one proton in the $1p_{3/2}$ shell. It is given by [12]

$$\Psi^{3/2}_{Li-7}=\frac{3}{\sqrt{15}}[\Psi_p^{3/2}\Psi_n^{3/2}\Psi_n^{-3/2}]-\frac{2}{\sqrt{15}}[\Psi_p^{3/2}\Psi_n^{1/2}\Psi_n^{-1/2}]$$
$$-\frac{1}{\sqrt{15}}[\Psi_p^{1/2}\Psi_n^{3/2}\Psi_n^{-1/2}]+\frac{1}{\sqrt{15}}[\Psi_p^{-1/2}\Psi_n^{3/2}\Psi_n^{1/2}]. \tag{5}$$

The superscripts refer to the z component of the total angular momentum. [. . .] stands for antisymmetrization. Four remaining nucleons occupy the $1s_{1/2}$ shell and their wave function is trivial. Being in the symmetric S state they do not contribute to the spin asymmetry. This nuclear wave function correctly describes the quantum numbers of the nucleus as $J^P=(\frac{3}{2})^-$ and predicts the correct value of the magnetic moment of ^{7}Li. In addition to the spin-angular dependence carried by the wave function (5) we have assumed a simple $|\vec{r}|$ dependence of the wave function (5)

$$|\Psi^{3/2}_{\rm Li-7}|^2\propto\exp\left(-\frac{3}{2}\frac{r^2}{R^2}\right) \tag{6}$$

with $R^2=5.7$ fm^2, which correctly reproduces the e.m. form factor of ^{7}Li.

In order to calculate the scattering cross section we form the usual Glauber series for the nuclear profile function and integrate it with the square of the nuclear wave function over positions of the nucleons. We have neglected the effects of Fermi motion of nucleons for shadowing since they are very small. For the details of the formalism see Appendix B.

We retain the first, second, and third terms of the expansion, which corresponds to single, double, and triple scattering of a projectile off the target. The contribution of the quadrupole term is negligible since already the triple scattering term gives only a less than 2% contribution. Since it is a fairly lengthy calculation, we refer the reader to Appendixes B and C for details of our calculations of the total cross section of the polarized effective hadronic state $|h\rangle$ with helicity + off polarized ^{7}Li with $M_J=3/2$ and with $M_J=-3/2$, which we named $\sigma_A^{+,3/2}$ and $\sigma_A^{+,-3/2}$.

Next, using Appendixes B and C, we find the difference of the cross sections with $M_J=3/2$ and $M_J=-3/2$

$$\Delta\sigma_A^{\mathrm{Li},3/2}=\sigma_A^{+,3/2}-\sigma_A^{+,-3/2}=\frac{13}{15}\Delta\sigma_p+\frac{2}{15}\Delta\sigma_n-\frac{\sigma_{\mathrm{eff}}}{\pi(R^2+3B)}\alpha_1\left(\frac{13}{15}\Delta\sigma_p+\frac{2}{15}\Delta\sigma_n\right)F(x)$$

$$-\frac{2\sigma_{\mathrm{eff}}}{\pi R^2}\left[\left(\frac{9}{15}\alpha_4+\frac{4}{15}\alpha_6\right)\Delta\sigma_p+\frac{2}{15}\alpha_6\Delta\sigma_n\right]F(x)+(\Delta\sigma_p 0.0143+\Delta\sigma_n 0.0025)g(x). \tag{7}$$

Here $\Delta\sigma_p=\sigma_p^{++}-\sigma_p^{+-}$ and $\Delta\sigma_n=\sigma_n^{++}-\sigma_n^{+-}$ are the differences of the $|h\rangle$-nucleon cross sections with parallel and antiparallel helicities for protons and neutrons, respectively. $F(x)=\exp(-(q_\parallel R)^2/3)=\exp(-176x^2)$ originates from the nonvanishing $q_\parallel$. $g(x)$ has the same origin. It is defined $g(0)=1$. Since it is a function of x slower than $F(x)$, in our numerical analysis we set $g(x)=1$ for any x without any loss of accuracy of our results. $B=6\ \mathrm{GeV}^{-2}$ is the slope of the $|h\rangle$-nucleon elastic cross section. $\alpha_1=1.376$, $\alpha_4=0.300$, $\alpha_6=0.402$. Since the triple scattering term has a complicated analytical structure, we simply give it in a numerical form [the last term in Eq. (7)]. Also note that the denominator of the fourth term in the expression above is $1/R^2$ rather than $1/(R^2+3B)$. We have omitted $3B$ as compared to R^2 to get an analytical expression. It does not change our predictions or numerical results. We point out that $\Delta\sigma_A^{\mathrm{Li},3/2}$ arises due to the orbital motion of the valence nucleons, which occupy the $1p_{3/2}$ shell.

When the target is longitudinally polarized with $M_J=1/2$ we can find the difference of the cross sections of the polarized effective state $|h\rangle$ off polarized ^{7}Li with $M_J=1/2$ and $M_J=-1/2$. Using Appendix D we obtain

$$\Delta\sigma_A^{\mathrm{Li},1/2}=\sigma_A^{+,1/2}-\sigma_A^{+,-1/2}=\frac{1}{3}\left\{\frac{13}{15}\Delta\sigma_p+\frac{2}{15}\Delta\sigma_n-\frac{\sigma_{\mathrm{eff}}}{\pi(R^2+3B)}\tilde{\alpha}_1\left(\frac{13}{15}\Delta\sigma_p+\frac{2}{15}\Delta\sigma_n\right)F(x)\right.$$

$$\left.-\frac{2\sigma_{\mathrm{eff}}}{\pi R^2}\left[\left(\frac{9}{15}\tilde{\alpha}_4+\frac{4}{15}\tilde{\alpha}_6\right)\Delta\sigma_p+\frac{2}{15}\tilde{\alpha}_6\Delta\sigma_n\right]F(x)+(\Delta\sigma_p 0.0139+\Delta\sigma_n 0.0015)g(x)\right\}. \tag{8}$$

Here $\tilde{\alpha}_1=4\alpha_2-\alpha_1=2.633$, $\tilde{\alpha}_4=(16\alpha_5-\alpha_4)/3=0.866$, $\tilde{\alpha}_6=4\alpha_5-\alpha_4=0.424$. From Eq. (8) one can see that $\Delta\sigma_A^{\mathrm{Li},1/2}$ is suppressed by approximately a factor of 3 as compared to $\Delta\sigma_A^{\mathrm{Li},3/2}$. Therefore, the measurement of $\Delta\sigma_A^{\mathrm{Li},1/2}$ and the extraction of the corresponding spin dependent structure function is not as feasible as that of $\Delta\sigma_A^{\mathrm{Li},3/2}$ and the corresponding spin dependent structure function. Hence, in our paper we will make predictions of the amount of shadowing and enhancement only for polarized ^{7}Li with $M_J=3/2$.

In deep inelastic scattering experiments one can measure the differential cross section of polarized projectiles off the longitudinally polarized target. The difference of such cross sections off the target polarized along the beam and in the opposite direction is called polarization asymmetry and it is proportional to the corresponding spin-dependent structure functions. On the other hand, the polarization asymmetry is proportional to the differences of the cross sections given by Eqs. (7) and (8). Therefore, in the Bjorken limit one can write [15]

$$\Delta\sigma_A^{\mathrm{Li},3/2}\propto\frac{d\sigma_A^{+,3/2}}{dx\,dy}-\frac{d\sigma_A^{+,-3/2}}{dx\,dy}=\frac{e^4M_AE}{2\pi Q^4}y(2-y)xg_1^{3/2\,3/2}(x),$$

$$\Delta\sigma_A^{\mathrm{Li},1/2}\propto\frac{d\sigma_A^{+,1/2}}{dx\,dy}-\frac{d\sigma_A^{+,-1/2}}{dx\,dy}=\frac{e^4M_AE}{2\pi Q^4}y(2-y)xg_1^{3/2\,1/2}(x). \tag{9}$$

Here $y=\nu/(M_AE)$, $x=Q^2/2\nu$, and $\nu=q\cdot P_A$. Since the spin of ^{7}Li is 3/2, one has to introduce two different spin-dependent structure functions $g_1^{3/2\,3/2}(x)$ and $g_1^{3/2\,1/2}(x)$. Note that the structure functions $g_2^{3/2\,3/2}(x)$ and $g_2^{3/2\,1/2}(x)$ are of higher twist and vanish in the Bjorken limit. In the quark parton language the spin-dependent structure functions $g_1^{3/2\,3/2}(x)$ and $g_1^{3/2\,1/2}(x)$ are defined [15]

$$g_1^{3/2\,3/2}(x)\equiv\frac{1}{2}[q_\uparrow^{3/2\,3/2}(x)-q_\downarrow^{3/2\,3/2}(x)],$$

$$g_1^{3/2\,1/2}(x)\equiv\frac{1}{2}[q_\uparrow^{3/2\,1/2}(x)-q_\downarrow^{3/2\,1/2}(x)], \tag{10}$$

where $q_\uparrow^{3/2\,M_J}(x)$ $(q_\downarrow^{3/2\,M_J}(x))$ is defined to be the probability to find a quark with momentum fraction x and spin up (down) in a target with spin component M_J. The sum over quark flavors is assumed.

We make our predictions of the amount of shadowing and enhancement for the nonsinglet combinations of the spin-dependent structure functions defined

$$g_{1A=7}^{n.s.\,3/2}(x,Q^2)\equiv g_1^{^7\mathrm{Li}\,3/2\,3/2}(x,Q^2)-g_1^{^7\mathrm{Be}\,3/2\,3/2}(x,Q^2),$$

$$g_{1A=7}^{n.s.\,1/2}(x,Q^2)\equiv g_1^{^7\mathrm{Li}\,3/2\,1/2}(x,Q^2)-g_1^{^7\mathrm{Be}\,3/2\,1/2}(x,Q^2),$$

$$g_{1A=1}^{n.s.}(x,Q^2)\equiv g_1^p(x,Q^2)-g_1^n(x,Q^2). \tag{11}$$

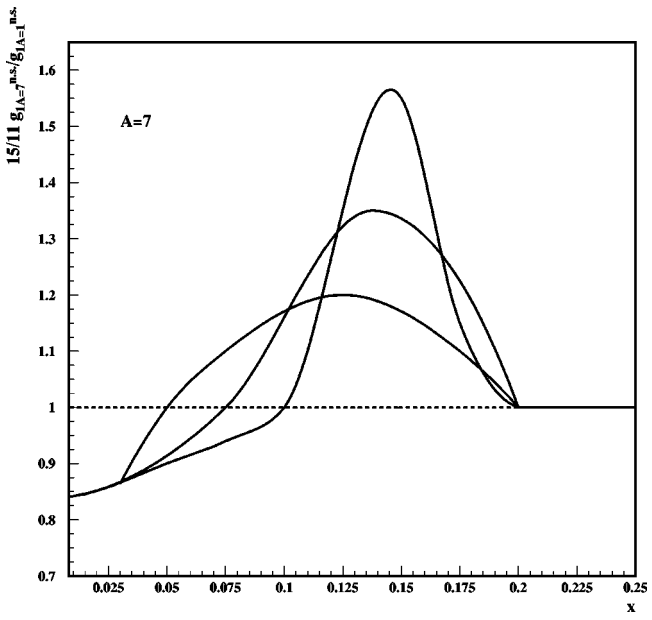

FIG. 1. $g_{1A=7}^{n.s.\ 3/2}(x,Q^2)/g_{1A=1}(x,Q^2)$ as a function of x. The straight-dashed line is the impulse approximation. The solid lines are a result of our calculation of shadowing and modeling of enhancement, which preserves R.

These nonsinglet combinations for $A=7$ are proportional to $\Delta\sigma_A^{\mathrm{Li},3/2}-\Delta\sigma_A^{\mathrm{Be},3/2}$ $(\Delta\sigma_A^{\mathrm{Li},1/2}-\Delta\sigma_A^{\mathrm{Be},1/2})$ by virtue of Eq. (9).

In order to get $\Delta\sigma_A^{\mathrm{Be},3/2}$ $(\Delta\sigma_A^{\mathrm{Be},1/2})$ from $\Delta\sigma_A^{\mathrm{Li},3/2}$ $(\Delta\sigma_A^{\mathrm{Li},1/2})$ one should simply substitute the valence proton by the valence neutron. Therefore, using Eq. (7) we obtain for the ratio of the nonsinglet structure functions with $A=7$ and $A=1$ for the nuclear target with $M_J=3/2$

$$\frac{g_{1A=7}^{n.s.\ 3/2}(x,Q^2)}{g_{1N}^{n.s.}(x,Q^2)} = \frac{\Delta\sigma_A^{\mathrm{Li},3/2}-\Delta\sigma_A^{\mathrm{Be},3/2}}{\Delta\sigma_p-\Delta\sigma_n} = \frac{11}{15}\times\left[1-\frac{\sigma_{\mathrm{eff}}}{\pi(R^2+3B)}\alpha_1 F(x) - \frac{2\sigma_{\mathrm{eff}}}{\pi R^2}\left(\frac{9}{15}\alpha_4+\frac{2}{15}\alpha_6\right)\frac{15}{11}F(x)+0.0161g(x)\right]. \quad (12)$$

Substituting $R^2=5.7$ fm^2, $\sigma_{\mathrm{eff}}=17$ mb, $B=6$ GeV^{-2}, and numerical values of α's we obtain

$$\frac{g_{1A=7}^{n.s.\ 3/2}(x,Q^2)}{g_{1A=1}^{n.s}(x,Q^2)} = \frac{11}{15}\times[1-0.177\exp(-176x^2) + 0.016g(x)]. \quad (13)$$

This equation is our main result for deep inelastic scattering on polarized ^{7}Li. It predicts 16% shadowing of $\frac{15}{11}\times g_{1A=7}^{n.s.\ 3/2}(x,Q^2)/g_{1A=1}^{n.s.}(x,Q^2)$ for $x\leqslant 10^{-2}$ (see the solid lines in Fig. 1).

When the target is polarized longitudinally with $M_J=1/2$, we obtain for the ratio of the corresponding nonsinglet structure function with $A=7$ and $A=1$

$$\frac{g_{1A=7}^{n.s.\ 1/2}(x,Q^2)}{g_{1N}^{n.s.}(x,Q^2)} = \frac{\Delta\sigma_A^{\mathrm{Li},1/2}-\Delta\sigma_A^{\mathrm{Be},1/2}}{\Delta\sigma_p-\Delta\sigma_n} = \frac{1}{3}\times\frac{11}{15}\times\left[1-\frac{\sigma_{\mathrm{eff}}}{\pi(R^2+3B)}\tilde{\alpha}_1 F(x) - \frac{2\sigma_{\mathrm{eff}}}{\pi R^2}\left(\frac{9}{15}\tilde{\alpha}_4+\frac{2}{15}\tilde{\alpha}_6\right)\frac{15}{11}F(x)+0.0372g(x)\right]. \quad (14)$$

Numerically Eq. (14) gives

$$\frac{g_{1A=7}^{n.s.\ 1/2}(x,Q^2)}{g_{1N}^{n.s.}(x,Q^2)} = \frac{1}{3}\times\frac{11}{15}\times[1-0.372\exp(-176x^2)+0.037g(x)]. \quad (15)$$

Comparing Eq. (15) with Eq. (13) one can see that the structure function $g_{1A=7}^{n.s.\ 1/2}(x,Q^2)$ is suppressed by approximately a factor of 3.5 in the region $x<0.05$ as compared to $g_{1A=7}^{n.s.\ 3/2}(x,Q^2)$. This makes it difficult to determine the structure function in the experiment.

Now we can prove our observation that this amount of shadowing for the polarized structure functions is larger by approximately a factor of 2 than that for the unpolarized one. In order to do so we first need to find the total scattering cross section of the unpolarized effective hadronic projectile $|h\rangle$ off the polarized ^{7}Li target with $M_J=3/2$ and $M_J=1/2$. We refer the reader to Appendix E for the details of this calculation. We define the scattering cross section of the unpolarized $|h\rangle$ off the unpolarized ^{7}Li target by

$$\sigma_A=\frac{1}{2}(\sigma_A^{3/2}+\sigma_A^{1/2}). \quad (16)$$

Here $\sigma_A^{3/2}$ and $\sigma_A^{1/2}$ are the scattering cross sections of the unpolarized $|h\rangle$ off the ^{7}Li target with $M_J=3/2$ and $M_J=1/2$, respectively. Then, using the results of Appendix E, we obtain for the ratio of scattering cross sections of the unpolarized effective state $|h\rangle$ off unpolarized ^{7}Li to $A\sigma_{\mathrm{eff}}$

$$\frac{\sigma_A}{7\sigma_{\mathrm{eff}}}=1-0.0996F(x)+0.0072g(x). \quad (17)$$

Equation (17) gives 9.2% shadowing at $x\leqslant 0.01$. Therefore, the amount of shadowing in the polarized case is larger by a factor of 2 than that for the unpolarized case with a high accuracy.

Semiquantitatively one can see the origin of this factor of 2 from the following idealized argument. Let us assume that

in ^{7}Li and ^{3}He all nuclear spin is due to the spin of a single valence nucleon. Then the Glauber expansion for the polarized target reads

$$\frac{\Delta\sigma_A}{\Delta\sigma_N}=1-(A-1)\frac{\sigma_{\rm eff}}{R^2}k+\cdots. \tag{18}$$

Here R^2 is the radius of the nucleus, k is some numerical factor. Note that in Eq. (18) we have kept only the first and the second terms since the higher terms are small. The factor $A-1$ originates from $A-1$ ways to couple the valence nucleon with the other nucleons. Equation (18) should be compared to

$$\frac{\sigma_A}{A\sigma_N}=1-\frac{A-1}{2}\frac{\sigma_{\rm eff}}{R^2}k+\cdots, \tag{19}$$

which describes shadowing in the case of the unpolarized target. Here σ_A is the total spin-averaged $|h\rangle$-nuclear cross section. $(A-1)/2$ comes from $A(A-1)/2$ ways to couple any two nucleons. One can see that in Eq. (19) the coefficient in front of the double scattering term is twice smaller than that in Eq. (18). Thus, in the idealized situation of one valence nucleon our observation of the enhancement of shadowing by a factor of 2 for the polarized target is a consequence of a simple counting of pairs.

For ^{3}He this idealization of one valence nucleon is a very good approximation since almost all nuclear spin is carried by the neutron. Consequently, in our calculations we used the wave function of ^{3}He, where only the neutron is polarized.

It is interesting to compare the ratio of the nonsinglet structure functions with $A=7$ and $M_J=3/2$ and $A=1$, given by Eq. (12), and the ratio of the spin-dependent structure functions $g_1^{3/2\,3/2}(x,Q^2)$ for ^{7}Li and a proton. The latter can be found immediately from Eq. (7)

$$\begin{aligned}\frac{g_1^{^7{\rm Li}\,3/2\,3/2}(x,Q^2)}{g_1^p(x,Q^2)}&=\frac{\Delta\sigma_A^{\rm Li}}{\Delta\sigma_p}=\frac{13}{15}+\frac{2}{15}\frac{\Delta\sigma_n}{\Delta\sigma_p}-\frac{\sigma_{\rm eff}}{\pi(R^2+3B)}\\&\times\alpha_1\left(\frac{13}{15}+\frac{2}{15}\frac{\Delta\sigma_n}{\Delta\sigma_p}\right)F(x)-\frac{2\sigma_{\rm eff}}{\pi R^2}\left[\left(\frac{9}{15}\alpha_4+\frac{4}{15}\alpha_6\right)\right.\\&\left.+\frac{2}{15}\alpha_6\frac{\Delta\sigma_n}{\Delta\sigma_p}\right]F(x)+\left(0.0143+\frac{\Delta\sigma_n}{\Delta\sigma_p}0.0025\right)\\&\times g(x).\end{aligned} \tag{20}$$

Although experimentally at $x\leqslant 0.05$ $g_{1p}(x,Q^2)$ is close to $-g_{1n}(x,Q^2)$, or $\Delta\sigma(p)$ is close to $-\Delta\sigma(n)$, we find the effect of this deviation to still be sizable. If we denote this deviation by some function $M(x)$ defined by

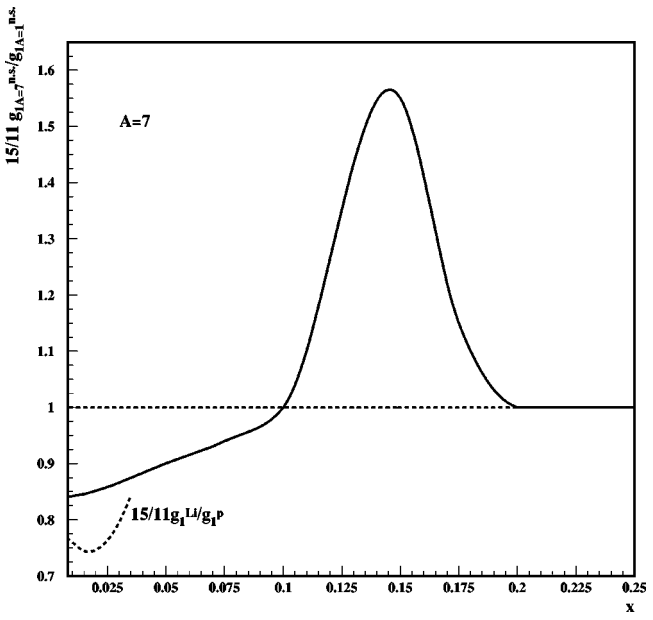

FIG. 2. $g_{1A=7}^{n.s.\,3/2}(x,Q^2)/g_{1A=1}^{n.s.}(x,Q^2)$ as a function of x. The straight-dashed line is the impulse approximation. The solid line is a result of our calculation of shadowing and modeling of enhancement, which preserves R. The curved-dashed line is $g_1^{\rm Li\,3/2\,3/2}(x,Q^2)/g_1^p(x,Q^2)$.

$$\frac{\Delta\sigma_n}{\Delta\sigma_p}=-1-M(x), \tag{21}$$

then we can present Eq. (20) in the form

$$\begin{aligned}\frac{g_1^{^7{\rm Li}\,3/2\,3/2}(x,Q^2)}{g_1^p(x,Q^2)}&=\frac{g_{1A=7}^{n.s.\,3/2}(x,Q^2)}{g_{1N}^{n.s.}(x,Q^2)}-M(x)[0.1333\\&-0.0257F(x)+0.0025g(x)].\end{aligned} \tag{22}$$

The first term is the ratio of nonsinglet spin-dependent structure functions presented by Eqs. (12) and (13). Shadowing for the ratio $g_1^{^7{\rm Li}\,3/2\,3/2}(x,Q^2)/g_1^p(x,Q^2)$ is presented by a curved dotted line in Fig. 2. We used the tabulation of the spin-dependent structure functions $g_{1A=1}^{n.s.}(x,Q_0^2)$, $g_1^p(x,Q_0^2)$ and $g_1^n(x,Q_0^2)$ at $Q_0^2=10$ GeV^2 from [16] based on the most recent analysis of the Spin Muon Collaboration (SMC) data.

The presence of nuclear shadowing in the spin-dependent structure function $g_1^{^7{\rm Li}\,3/2\,3/2}(x,Q^2)$ violates the relation, which follows from the Bjorken sum rule [9]

$$\begin{aligned}R&=\frac{\int_0^1[g_1^{^7{\rm Li}\,3/2\,3/2}(x,Q^2)-g_1^{^7{\rm Be}\,3/2\,3/2}(x,Q^2)]dx}{\int_0^1[g_1^p(x,Q^2)-g_1^n(x,Q^2)]dx}\\&=\frac{g_A(A=7)}{g_A(A=1)},\end{aligned} \tag{23}$$

where g_A is the axial coupling constant for β decay.

Note that the main difference between $g_A(A=7)$ and $g_A(A=1)$, i.e., between $g_{1A=7}^{n.s.\ 3/2}(x,Q^2)$ and $g_{1A=1}^{n.s.}(x,Q^2)$, is caused by the orbital motion of valence nucleons, which occupy the $1p_{3/2}$ shell. This gives the factor $11/15=0.73$. Nuclear shadowing at small x decreases this value by an additional 16%. Addition quenching of R by a factor of $\eta_A=0.91$ [17] is caused by higher partial waves in the ^{7}Li ground-state wave function as well as admixtures of nonnucleonic degrees of freedom.

We suggest to model the $x\sim 0.1$ enhancement so that its contribution to R compensates shadowing effect in the Bjorken sum rule. We require that

(i) enhancement does not affect the region $x\leqslant 0.05$, where shadowing is saturated.

(ii) enhancement is concentrated at $0.2\geqslant x\geqslant 0.05(0.1)$ and compensates shadowing at $x\approx 0.1$:

$$\frac{15}{11}\int_0^{0.2} dx[g_1^{^7\mathrm{Li}\ 3/2\ 3/2}(x,Q^2)-g_1^{^7\mathrm{Be}\ 3/2\ 3/2}(x,Q^2)] = \int_0^{0.2} dx[g_1^p(x,Q^2)-g_1^n(x,Q^2)]. \quad (24)$$

The shape of the curve, which describes the enhancement region, deserves a special discussion. We model enhancement according to our expectations suggested by experimental data on the x dependence of the European Muon Collaboration effect. While we know that shadowing extends to $x\approx 0.05$, it is not known where the cross over point from shadowing to enhancement lies. While equality (24) fixes the integrated contribution of enhancement, we can only guess how enhancement is distributed along x, or where it reaches the maximum. Since the main contribution to the nuclear shadowing in Eq. (24) comes from the region $x\leqslant 0.03$–0.05, the variation of the crossover point between $x=0.05$ and $x=0.1$ does not change significantly the contribution of shadowing to the integral (24). It only governs the spread of enhancement in x and its height.

We model enhancement at normalization point $Q^2=4$ GeV^2 according to Eq. (24). To obtain it at larger Q^2 one has to use the QCD evolution of the spin-dependent parton densities. However, since the scaling violation between $Q^2=4$ GeV^2 and $Q^2=10$ GeV^2 is small we used the SMC parametrization of the nonsinglet structure function $g_{1A=1}^{n.s}(x,Q_0^2)$ from [16] at $Q^2=10$ GeV^2. Hence, we discuss here only the predictions for $g_{1A=7}^{n.s\ 3/2}(x,Q_0^2)$ at $Q^2=4$–10 GeV^2.

Note also that although the parametrization of the parton densities of [16] is limited by $x=0.003$, the contribution to the integral from the region $x<0.003$ is very small. Therefore, in our numerical modeling of enhancement in integral (24) the lower limit of integration was $x=0.003$.

Our results are presented in Figs. 1 and 2. The solid lines in Fig. 1 represent three possible scenarios of $15/11\times g_{1A=7}^{n.s.\ 3/2}(x,Q^2)/g_{1A=1}^{n.s.}(x,Q^2)$ with the crossover points $x=0.05$, 0.075, and 0.1 as functions of x. Enhancement is modeled so that both nuclear shadowing and enhancement do not alter R. The choice of the crossover point changes the peak value of enhancement considerably. We obtained 55% shadowing at $x=0.15$ for the crossover point $x=0.1$, 42% shadowing at $x=0.138$ for the crossover point $x=0.075$, and 20% shadowing at $x=0.125$ for the crossover point $x=0.05$.

In Fig. 2 we present one of the curves of $15/11\times g_{1A=7}^{n.s.\ 3/2}(x,Q^2)/g_{1A=1}^{n.s.}(x,Q^2)$ from Fig. 1. The curved dotted line is our calculation of shadowing for the ratio $15/11\times g_1^{^7\mathrm{Li}\ 3/2\ 3/2}(x,Q^2)/g_1^p(x,Q^2)$. The difference between the solid and dotted lines illustrated that at low x shadowing is different for $g_{1A=7}^{n.s.\ 3/2}(x,Q^2)/g_{1A=1}^{n.s.}(x,Q^2)$ and $g_1^{^7\mathrm{Li}\ 3/2\ 3/2}(x,Q^2)/g_1^p(x,Q^2)$ due to a nonvanishing difference between $g_{1p}(x,Q^2)$ and $-g_{1n}(x,Q^2)$.

Note that in both figures we have not taken into account the quenching factor $\eta_A=0.91$ determined from the g_A measurements. In order to reflect this quenching the ratio $g_{1A=7}^{n.s.\ 3/2}(x,Q^2)/g_{1A=1}^{n.s}(x,Q^2)$ has to be multiplied by $\eta_A=0.91$.

From Figs. 1 and 2 one can see that there are sizable nuclear effects at $10^{-4}\leqslant x\leqslant 0.2$ in the ratio of the spin-dependent structure functions $g_{1A=7}^{n.s.\ 3/2}(x,Q^2)/g_{1A=1}^{n.s.}(x,Q^2)$. These effects have a nontrivial x dependence: 16% shadowing for $10^{-4}\leqslant x\leqslant 0.03$ and enhancement of an order of 20 (55)% at $x\approx 0.125$ (0.15), if enhancement occupies the region $0.05\leqslant x\leqslant 0.2$ $(0.1\leqslant x\leqslant 0.2)$.

III. HOW THE MANY-NUCLEON DESCRIPTION BREAKS DOWN

It is interesting that our analysis of the spin-dependent structure function of ^{7}Li $g_1^{^7\mathrm{Li}\ 3/2\ 3/2}(x,Q^2)$ in a wide range of $0.2>x>10^{-3}$ shows how the many-nucleon description of ^{7}Li becomes invalid. We shall show that one cannot describe deep inelastic scattering off polarized ^{7}Li as scattering off a many-nucleon system. Therefore, one needs to introduce explicitly nonnucleonic degrees of freedom to explain the behavior $g_1^{^7\mathrm{Li}\ 3/2\ 3/2}(x,Q^2)$. Our proof is based on the following observation. If the many-nucleon description breaks down, the following inequality holds:

$$g_1^{^7\mathrm{Li}\ 3/2\ 3/2}(x,Q^2)\neq a g_1^p(x,Q^2)+b g_1^n(x,Q^2). \quad (25)$$

Here a and b are some numerical factors, which in the impulse approximation [Eq. (4)] are equal to the polarizations of the valence proton and neutron. They are also constrained by the Bjorken sum rule for $A=7$ system which leads to

$$\frac{15}{11}(a-b)=g_{A=7}/g_{A=1}=0.91. \quad (26)$$

The factor a is much larger than b since the neutron contribution to the spin of ^{7}Li is small. Although corrections to the nuclear shell model might change the coefficients a and b, it will definitely not be enough to turn Eq. (25) into an equality.

Since nuclear shadowing for the ratio $g_1^{^7\mathrm{Li}\ 3/2\ 3/2}(x,Q^2)/[13/15 g_1^p(x,Q^2)+2/15 g_1^n(x,Q^2)]$ is the

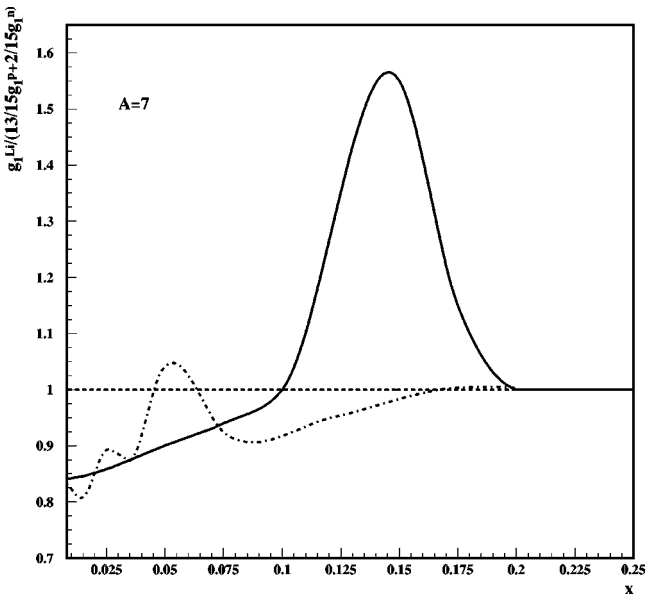

FIG. 3. $g_1^{^7\mathrm{Li}\,3/2\,3/2}(x,Q^2)/[13/15\,g_1^p(x,Q^2)+2/15 g_1^n(x,Q^2)]$ as a function of x. The solid line is a result of our calculation of shadowing and modeling of enhancement, which preserves R. The dashed-dotted line is given by Eq. (27).

same as for $15/11 g_{1A=7}^{n.s.\,3/2}(x,Q^2)/g_{1A=1}^{n.s.}(x,Q^2)$ with a very high accuracy, see Eq. (12), we will make a realistic assumption that enhancement is also equal for both ratios. Then if we rewrite Eq. (25) in the form

$$\frac{g_1^{^7\mathrm{Li}\,3/2\,3/2}(x,Q^2)}{[13/15 g_1^p(x,Q^2)+2/15 g_1^n(x,Q^2)]} \neq \frac{1}{g_1^p(x,Q^2)+2/11\,g_1^D(x,Q^2)}[a' g_1^p(x,Q^2) + b' g_1^D(x,Q^2)], \tag{27}$$

we can immediately compare its predictions with our predictions for enhancement given by the solid line in Figs. 1 and 2. In Eq. (27) we used the deuteron spin-dependent structure function $g_1^D(x,Q^2)=g_1^p(x,Q^2)+g_1^n(x,Q^2)$, $a'=15/11(a-b)$ and $b'=15/11 b$. To obtain the best fit to nuclear shadowing by Eq. (27) we have chosen $a'=0.90$ and $b'=0.38$.

In Fig. 3 we plot the ratio $g_1^{^7\mathrm{Li}\,3/2\,3/2}(x,Q^2)/[13/15\,g_1^p(x,Q^2)+2/15\,g_1^n(x,Q^2)]$ as a function of x. The solid curved line is the same as in Fig. 2. The dash-dotted line is given by Eq. (27). The clear inconsistency of both proves that inequality (25) is valid, or that one cannot describe the discussed process with ^{7}Li as with a many-nucleon system. If the many-nucleon description worked, $g_1^{^7\mathrm{Li}\,3/2\,3/2}(x,Q^2)$ could be approximated quite well by the right-hand side of Eq. (25). Due to the presence of enhancement at $0.05\ (0.1)\leqslant x\leqslant 0.2$ it is clearly impossible.

Therefore, in order to test the discussed ideas in experiment, one should explore the region of enhancement $0.05\ (0.1)\leqslant x\leqslant 0.2$, where the many-nucleon description of polarized deep inelastic scattering off ^{7}Li with $M_J=3/2$ is expected to break down completely.

IV. DIFFERENCES IN SCATTERING OF UNPOLARIZED LEPTONS OFF ^{7}Li WITH $M_J=3/2$ AND $M_J=1/2$

As a by-product of our calculations we notice that one can see in experiment the difference in cross sections of deep inelastic scattering of unpolarized leptons off ^{7}Li polarized longitudinally with $M_J=3/2$ and $M_J=1/2$. Combining Eqs. (E4) and (E6) of Appendix E we obtain

$$\frac{\sigma_A^{3/2}-\sigma_A^{1/2}}{\sigma_{\mathrm{eff}}}=-0.1029F(x)-0.0154g(x), \tag{28}$$

which suggests a 12% effect at $x\leqslant 0.01$. Although the quantity, which can be measured in experiment, is the ratio of $\sigma_A^{3/2}-\sigma_A^{1/2}$ to the unpolarized cross section σ_A. Combining Eqs. (28) and (17) we find that at $x\leqslant 0.01$

$$\frac{\sigma_A^{3/2}-\sigma_A^{1/2}}{\sigma_A}=-0.0186. \tag{29}$$

Therefore, we predict a 2% effect in the difference of scattering cross sections of deep inelastic scattering of unpolarized leptons off ^{7}Li with $M_J=3/2$ and $M_J=1/2$. This effect is due to the presence of higher partial waves in the wave function of ^{7}Li. Note that a similar effect was pointed out for deuterium [10,18–20].

V. NUCLEAR EFFECTS AT SMALL x IN $g_{1A}(x,Q^2)$ FOR ^{3}He

Another remarkable nucleus, which suits well for the purpose of studying spin-dependent structure functions, is ^{3}He. Nuclear polarization is carried predominantly by a single nucleon, the neutron, which enhances nuclear effects of shadowing and enhancement in two times as compared to the unpolarized nucleus. Below we will give a short account of our original paper [9], where more details and references can be found.

Using the modified Gribov-Glauber formalism we presented the total cross section of the polarized hadronic state $|h\rangle$ with helicity $+$ on polarized ^{3}He with helicity $\pm$ at $x\leqslant 0.05$

$$\sigma_A^{+,\pm}=\sigma_n^{+,\pm}+2\sigma_{\mathrm{eff}}-\frac{\sigma_{\mathrm{eff}}^2 e^{-\alpha q_\parallel^2}}{8\pi(\alpha+B)}-\frac{\sigma_n^{+,\pm}\sigma_{\mathrm{eff}} e^{-\alpha q_\parallel^2}}{4\pi(\alpha+B)} + \frac{\sigma_{\mathrm{eff}}^2\sigma_n^{+,\pm}}{48\pi^2(\alpha+B)^2}f(x), \tag{30}$$

where superscripts $++$ and $+-$ stand for parallel and anti-

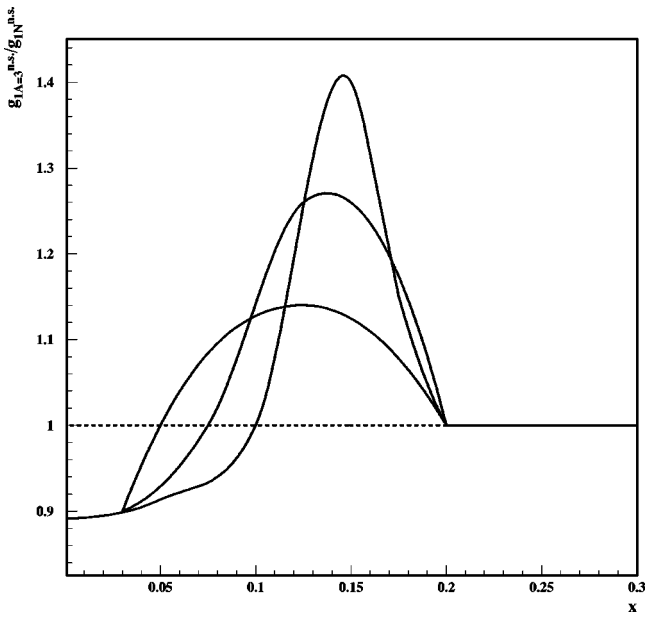

FIG. 4. $g_{1A=3}^{n.s.}(x,Q^2)/g_{1A=1}(x,Q^2)$ as a function of x. The straight-dashed line is the impulse approximation. The solid lines are a result of our calculation of shadowing and modeling of enhancement, which preserves R.

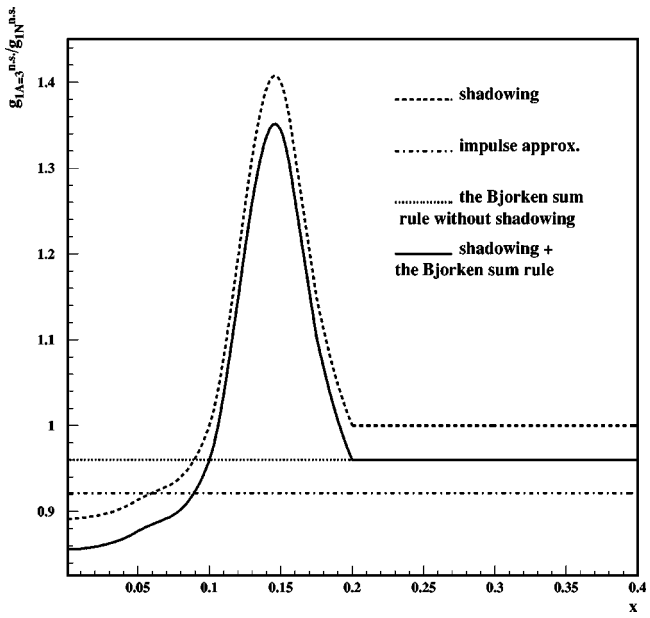

FIG. 5. $g_{1A=3}^{n.s.}(x,Q^2)/g_{1N}^{n.s.}(x,Q^2)$ as a function of x. The dashed line represents nuclear shadowing at small x and enhancement. The solid line is the result of the fit constrained to preserve the Bjorken sum rule.

parallel helicities of the incoming photon (the effective state h has the same helicity) and the target nucleus or the neutron. Here $\alpha=27$ GeV^{-2} is the slope of a nuclear one-particle density chosen to reproduce the e.m. form factor of ^{3}He. $B=6$ GeV^{-2} is the slope of the $|h\rangle$-nucleon cross section. The function $f(x)$ is a function of x slower than $\exp(-\alpha q_\parallel^2)$.

This leads to the ratio of the spin-dependent structure functions of ^{3}He and a neutron [9]

$$\frac{g_1^{^3\mathrm{He}}(x,Q_0^2)}{g_1^n(x,Q_0^2)}=\frac{\sigma_A^{+,+}-\sigma_A^{+,-}}{\sigma_n^{+,+}-\sigma_n^{+,-}}=1-\frac{\sigma_{\mathrm{eff}}e^{-\alpha q_\parallel^2}}{4\pi(\alpha+B)}+\frac{\sigma_{\mathrm{eff}}^2}{48\pi^2(\alpha+B)^2}f(x). \tag{31}$$

Numerically, for example at $x\leqslant 0.03$ $g_1^{^3\mathrm{He}}(x,Q_0^2)/g_{1^n}(x,Q_0^2)=0.9$, which provides the amount of nuclear shadowing, which is by a factor of 2 larger than the corresponding amount for unpolarized structure functions, $F_{2A=3}(x,Q^2)/3F_{2N}(x,Q^2)=0.95$.

Exactly as in the case of ^{7}Li we model enhancement so that its contribution to R compensates shadowing. We present our results in Figs. 4 and 5. These figures are somewhat different from the original figure presented in [9], where the x dependence of proton and neutron spin-dependent structure functions was not properly taken into account. Here we used the most recent parametrization from [16].

We plot $g_{1A=3}^{n.s.}(x,Q^2)/g_{1N}^{n.s.}(x,Q^2)=[g_1^{^3\mathrm{He}}(x,Q^2)-g_1^{^3\mathrm{H}}(x,Q^2)]/[g_1^n(x,Q^2)-g_1^p(x,Q^2)]$ as a function of x. Unlike ^{7}Li, since we assumed that only one nucleon carries all nuclear polarization, shadowing is the same for the ratios $g_1^{^3\mathrm{He}}(x,Q^2)/g_1^n(x,Q^2)$, $g_1^{^3\mathrm{He}}(x,Q^2)/g_1^p(x,Q^2)$ and $g_{1A=3}^{n.s.}(x,Q^2)/g_{1N}^{n.s.}(x,Q^2)$. In Fig. 4 we present three possible scenarios of enhancement, which depend on the crossover point, like in the case of ^{7}Li.

We obtained 40% enhancement at $x=0.15$ for the crossover point $x=0.1$, 26% enhancement at $x=0.138$ for the crossover point $x=0.075$ and 14% enhancement at $x=0.125$ for the crossover point $x=0.05$.

In Fig. 5 the dash-dotted straight line represents the ratio R in the impulse approximation, which includes also higher partial waves (S', D, etc.) in the ground-state wave function of ^{3}He. It corresponds to the x independent ratio of the spin-dependent structure functions $g_{1A=3}^{n.s.}(x,Q^2)/g_{1N}^{n.s.}(x,Q^2)=0.9215$. The dotted straight line represents R within the impulse approximation corrected to include non-nucleonic degrees of freedom in the ground-state wave function of ^{3}He. It corresponds to $g_{1A=3}^{n.s.}(x,Q^2)/g_{1N}^{n.s.}(x,Q^2)=0.9634$. The curved dotted line is a result of our calculations of nuclear shadowing and modeling of enhancement. We assume that the discussed effects contribute multiplicatively, which shifts the curved dotted line downward. Our predictions for $g_{1A=3}^{n.s.}(x,Q^2)/g_{1N}^{n.s.}(x,Q^2)$, $g_1^{^3\mathrm{He}}(x,Q^2)/g_1^n(x,Q^2)$ and $g_1^{^3\mathrm{H}}(x,Q^2)/g_1^p(x,Q^2)$ are given by the solid line.

We conclude that similar to ^{7}Li, nuclear effects at $10^{-4}\leqslant x\leqslant 0.2$ in the ratio of the spin-dependent nuclear structure functions $g_{1A=3}^{n.s.}(x,Q^2)/g_{1N}^{n.s.}(x,Q^2)$ are large: shadowing is of an order of 10% for $10^{-4}\leqslant x\leqslant 0.03$ and enhancement is of an order of 14 (40)% at $x\approx 0.125$ (0.15), if enhancement occupies the region $0.05\leqslant x\leqslant 0.2$ $(0.1\leqslant x\leqslant 0.2)$.

VI. NUCLEAR SHADOWING FOR POLARIZED GLUONS FOR ^{3}He

As we pointed out in Sec. II the nuclear shadowing in the gluon channel is larger by a factor of three than that in the quark channel. Although the contribution of the gluon channel to the polarized DIS has not received a solid experimental ground, we still can make a prediction for the amount of nuclear shadowing for the polarized nuclear gluon parton density $\Delta G_A(x,Q^2)$. Similarly to Eq. (31) one can estimate the amount of nuclear shadowing for $\Delta G_A(x,Q^2)$ for ^{3}He, see also [2],

$$\frac{\Delta G_A(x,Q^2)}{\Delta G_N(x,Q^2)}=1-\frac{\sigma_{\rm eff}\,e^{-\alpha\overline{q_\parallel}^2}}{4\pi(\alpha+B)}+\frac{\sigma_{\rm eff}^2}{48\pi^2(\alpha+B)^2}f(x). \tag{32}$$

Here $\Delta G_N(x,Q^2)$ is the polarized nucleon gluon parton density.

The longitudinal momentum transferred to the nucleus is $\overline{q_\parallel}=(Q^2+\overline{M}^2)/2\nu$, where $\overline{M}$ is some typical mass of hadronic fluctuations in the photon wave function, which contain gluons. In the case of shadowing in the singlet quark and gluon channels, the relevant masses $\overline{M}$ can be related to the β shapes of the corresponding diffractive quark $q_{\rm diff}(\beta,Q^2,x_P,t)$ and gluon $g_{\rm diff}(\beta,Q^2,x_P,t)$ parton densities. $\beta=x/x_P$ is the fraction of the Pomeron momentum carried by the struck quark or gluon; x_P is the fraction of the proton momentum carried by the Pomeron. The recent analyses of the HERA data indicate that for low $Q_0^2\sim 4$ GeV^2 the shapes of diffractive quark and gluon parton densities are very similar [21]. Therefore, at low $Q_0^2\sim 4$ GeV^2, the typical masses $\overline{M}$ and the longitudinal momenta $\overline{q_\parallel}$ relevant for nuclear shadowing in the singlet quark and gluon channels are similar, which leads to an expectation of the onset of nuclear shadowing for similar x in the quark and gluon channels. However, with an increase of Q^2 due to the scaling violation, the gluon diffractive distribution broadens more strongly than the quark diffractive distribution, leading to a stronger shift of shadowing to smaller x in the gluon case. Hence, one may expect that for $Q^2\sim Q_0^2\sim 4$ GeV^2 the saturation of nuclear shadowing will occur at similar x for the quark and gluon channels, while at large Q^2, where the QCD evolution is important, the saturation of nuclear shadowing for the gluon channel will occur at smaller x than that for the quark channel. Since in this paper we consider relatively low Q^2, we expect that the saturation of nuclear shadowing for the polarized gluons [the ratio $\Delta G_A(x,Q^2)/\Delta G_N(x,Q^2)$] will take place at x similar to x for the polarized quark channel [the ratio $g_1^{^3{\rm He}}(x,Q_0^2)/g_1^n(x,Q_0^2)$].

Using $\sigma_{\rm eff}=50$ mb in Eq. (32) we will find at $x\leqslant 0.01$, where nuclear shadowing for the polarized gluons is expected to be saturated,

$$\frac{\Delta G_A(x,Q^2)}{\Delta G_N(x,Q^2)}=0.70. \tag{33}$$

This means that the effect of nuclear shadowing for polarized gluons for ^{3}He is of an order of 30%. In the future it may be possible to measure this effect at HERA when polarized protons are used.

VII. CONCLUSIONS

We propose to use polarized nuclear targets of ^{7}Li and ^{3}He for studying nuclear effects in the spin-dependent structure functions $g_{1A}(x,Q^2)$, where these effects are expected to be enhanced by a factor of 2 as compared to the unpolarized targets. We predict a significant x dependence at $10^{-4}\leqslant x\leqslant 0.2$ due to the effects of nuclear shadowing and enhancement. The effect of nuclear shadowing is of an order of 16% for the ratio $g_{1A=7}^{n.s.}(x,Q^2)/g_{1N}^{n.s.}(x,Q^2)$ and 10% for $g_{1A=3}^{n.s.}(x,Q^2)/g_{1N}^{n.s.}(x,Q^2)$. By imposing the requirement that the Bjorken sum rule is satisfied we model the effect of enhancement. We find the effect of enhancement at $x\approx 0.125$ (0.15) to be of an order of 20 (55)% for $g_{1A=7}^{n.s.}(x,Q^2)/g_{1N}^{n.s.}(x,Q^2)$ and 14 (40)% for $g_{1A=3}^{n.s.}(x,Q^2)/g_{1N}^{n.s.}(x,Q^2)$. We also point out that since the discussed nuclear effects in ^{3}He are quite sizable, one should take them into account when extracting the neutron spin-dependent structure function from ^{3}He data.

We predict even larger nuclear shadowing effect for the polarized gluon densities for ^{3}He.

We predict a 2% effect in the difference of scattering cross sections of deep inelastic scattering of unpolarized leptons off ^{7}Li longitudinally polarized with $M_J=3/2$ and $M_J=1/2$. As in the deuteron, this effect is attributed to the presence of higher partial waves in the wave function of ^{7}Li.

We also predict a gross deviation from the many-nucleon description of deep inelastic scattering off ^{7}Li. The effect is pronounced in the enhancement region $0.2>x>0.05$, where we suggest studying it experimentally.

ACKNOWLEDGMENTS

M.S. would like to thank DESY for the hospitality during the time this work was done. We thank D. Crabb, L. Frankfurt, J. Lichtenstadt, and W. Weise for useful discussions. This work was supported in part by the U.S. Department of Energy.

APPENDIX A: THE GROUND-STATE WAVE FUNCTION OF ^{7}Li WITH $M_J=3/2,\ 1/2,\ -1/2,\ -3/2$

The spin of ^{7}Li is 3/2. In the shell model the ground-state wave function of ^{7}Li with the z component of the total angular momentum $M_J=3/2$ is given by [12]

$$\Psi_{Li-7}^{3/2}=\frac{3}{\sqrt{15}}[\Psi_p^{3/2}\Psi_n^{3/2}\Psi_n^{-3/2}]-\frac{2}{\sqrt{15}}[\Psi_p^{3/2}\Psi_n^{1/2}\Psi_n^{-1/2}]$$
$$-\frac{1}{\sqrt{15}}[\Psi_p^{1/2}\Psi_n^{3/2}\Psi_n^{-1/2}]+\frac{1}{\sqrt{15}}[\Psi_p^{-1/2}\Psi_n^{3/2}\Psi_n^{1/2}]. \tag{A1}$$

In order to find the wave function of ^{7}Li with $M_J=1/2$ we act upon the wave function with $M_J=3/2$ by the lowering operator L_-. Using the relations

$$L_-\Psi^{3/2}=\sqrt{3}\Psi^{1/2},$$

$$L_-\Psi^{1/2}=2\Psi^{-1/2},$$

$$L_-\Psi^{-1/2}=\sqrt{3}\Psi^{-3/2},$$

$$L_-\Psi^{-3/2}=0, \tag{A2}$$

we obtain the nuclear wave function with $M_J=1/2$

$$\Psi^{1/2}_{Li-7}=\frac{1}{\sqrt{15}}[\Psi_p^{3/2}\Psi_n^{1/2}\Psi_n^{-3/2}]+\frac{2}{\sqrt{15}}[\Psi_p^{1/2}\Psi_n^{3/2}\Psi_n^{-3/2}]$$
$$-\frac{3}{\sqrt{15}}[\Psi_p^{1/2}\Psi_n^{1/2}\Psi_n^{-1/2}]+\frac{1}{\sqrt{15}}[\Psi_p^{-3/2}\Psi_n^{3/2}\Psi_n^{1/2}]. \tag{A3}$$

In a similar way we obtain the ground-state wave function of ^{7}Li with $M_J=-1/2$

$$\Psi^{-1/2}_{Li-7}=\frac{1}{\sqrt{15}}[\Psi_p^{3/2}\Psi_n^{-1/2}\Psi_n^{-3/2}]+\frac{2}{\sqrt{15}}[\Psi_p^{-1/2}\Psi_n^{3/2}\Psi_n^{-3/2}]$$
$$-\frac{3}{\sqrt{15}}[\Psi_p^{-1/2}\Psi_n^{1/2}\Psi_n^{-1/2}]+\frac{1}{\sqrt{15}}[\Psi_p^{-3/2}\Psi_n^{3/2}\Psi_n^{-1/2}] \tag{A4}$$

and with $M_J=-3/2$

$$\Psi^{-3/2}_{Li-7}=\frac{3}{\sqrt{15}}[\Psi_p^{-3/2}\Psi_n^{3/2}\Psi_n^{-3/2}]-\frac{2}{\sqrt{15}}[\Psi_p^{-3/2}\Psi_n^{1/2}\Psi_n^{-1/2}]$$
$$-\frac{1}{\sqrt{15}}[\Psi_p^{-1/2}\Psi_n^{1/2}\Psi_n^{-3/2}]$$
$$+\frac{1}{\sqrt{15}}[\Psi_p^{1/2}\Psi_n^{-1/2}\Psi_n^{-3/2}]. \tag{A5}$$

APPENDIX B: SCATTERING OFF POLARIZED ^{7}Li TARGETS WITH $M_J=3/2$ AND $M_J=-3/2$. SINGLE AND DOUBLE SCATTERING

In this appendix we will give detailed calculations of the total scattering cross section of a polarized incoming hadron with helicity + off a polarized target of ^{7}Li with the z component of the total angular momentum $M_J=3/2$ and $M_J=-3/2$. When $M_J=3/2$ the target is polarized along the beam polarization. If $M_J=-3/2$ the target is polarized in the direction opposite to the beam polarization.

We used the modified Glauber-Gribov formalism. In this formalism the total nuclear cross section σ_A is related to the nuclear profile function $\Gamma_A(\vec{b})$ as

$$\sigma_A=2\,\mathrm{Re}\int d^2\vec{b}\,\Gamma_A(\vec{b}). \tag{B1}$$

Here $\vec{b}$ is the impact parameter of the incoming particle with respect to the center of mass of the target nucleus. The nuclear profile function can be expanded as a series over nucleon profile functions $\Gamma(\vec{b}-\vec{s_i})$, where $\vec{s_i}$ is the transverse position of an ith nucleon. In the series we will keep only single, double, and triple terms in accordance with our observation that higher terms give a negligible contribution in our case

$$\Gamma_A(\vec{b})=\langle\Psi^{3/2}_{\mathrm{Li}-7}|\sum_{i=1}^{7}\Gamma(\vec{b}-\vec{s_i})+\sum_{i=1,j>i}^{7}\Gamma(\vec{b}-\vec{s_i})$$
$$\times\Gamma(\vec{b}-\vec{s_j})\Theta(z_j-z_i)e^{iq_\parallel(z_i-z_j)}$$
$$-\sum_{i=1,j>i,k>j}^{7}\Gamma(\vec{b}-\vec{s_i})\Gamma(\vec{b}-\vec{s_j})\Gamma(\vec{b}-\vec{s_k})$$
$$\times\Theta(z_j-z_i)\Theta(z_k-z_j)e^{iq_\parallel(z_i-z_k)}|\Psi^{3/2}_{\mathrm{Li}-7}\rangle. \tag{B2}$$

Note that the series is averaged with the ground-state wave function $\Psi^{3/2}_{\mathrm{Li}-7}$.

This formula is different from the usual Glauber series. The exponents account for a nonzero $q_\parallel$. The θ functions fix time ordering of elementary scattering processes. The numerical factors in front of the second and third terms are used because there are two ways to time order a pair of nucleons and there are six ways to time order three nucleons.

The nucleon profile function is related to the scattering amplitude $f(\vec{k_t})$

$$\Gamma(\vec{b}-\vec{s_i})=\frac{1}{2\pi ik_t}\int d^2\vec{k_t}e^{i\vec{k_t}(\vec{b}-\vec{s_i})}f(\vec{k_t}). \tag{B3}$$

The scattering amplitude at high energies is predominantly imaginary

$$f(\vec{k_t})=\frac{ik}{4\pi}\sigma e^{-B/2k_t^2}. \tag{B4}$$

Here B is the slope of the hadron-nucleon cross section, σ is the hadron-nucleon cross section.

Combining Eqs. (B3) and (B4) we obtain the nucleon profile function as a function of the nucleon transverse coordinates $\vec{s_i}$

$$\Gamma(\vec{b}-\vec{s_i})=\frac{\sigma}{4\pi B}e^{-(\vec{b}-\vec{s_i})^2/2B}. \tag{B5}$$

We used this expression of the nucleon profile function in series (B2). We have neglected effects of Fermi motion of nucleons in the nucleus since these effects are negligible at $x<0.5$. Next we will deal with single, double, and triple terms of this series.

Single scattering. We are computing $\sigma_A^{+,3/2}$, the total

scattering cross section of a hadronic projectile with helicity + off a target of ^{7}Li with $M_J=3/2$. The contribution of four nonvalence nucleons in the $1s_{1/2}$ shell is simply $4\sigma_{\rm eff}$. The contribution of the three valence nucleons is governed by the wave function (5). Since each valence nucleon belongs to the $1p_{3/2}$ shell, its total angular momentum is 3/2. Then, the spin-angular wave function of a valence nucleon with the z component of the total angular momentum $m_j=3/2$, 1/2, $-1/2$ or $-3/2$ is

$$\Psi_N^{3/2}=Y_{11}(\theta,\phi)|\uparrow\rangle=-\sqrt{\frac{3}{8\pi}}\sin\theta e^{i\phi}|\uparrow\rangle,$$

$$\Psi_N^{1/2}=\frac{1}{\sqrt{3}}Y_{11}(\theta,\phi)|\downarrow\rangle+\sqrt{\frac{2}{3}}Y_{10}(\theta,\phi)|\uparrow\rangle$$

$$=-\frac{1}{\sqrt{8\pi}}\sin\theta e^{i\phi}|\downarrow\rangle+\frac{1}{\sqrt{2\pi}}\cos\theta|\uparrow\rangle,$$

$$\Psi_N^{-1/2}=\sqrt{\frac{2}{3}}Y_{10}(\theta,\phi)|\uparrow\rangle+\frac{1}{\sqrt{3}}Y_{1-1}(\theta,\phi)|\downarrow\rangle$$

$$=+\frac{1}{\sqrt{2\pi}}\cos\theta|\uparrow\rangle-\frac{1}{\sqrt{8\pi}}\sin\theta e^{-i\phi}|\downarrow\rangle,$$

$$\Psi_N^{-3/2}=Y_{1-1}(\theta,\phi)|\downarrow\rangle=\sqrt{\frac{3}{8\pi}}\sin\theta e^{-i\phi}|\downarrow\rangle. \quad \text{(B6)}$$

Here the superscripts stand for m_J. θ is the polar angle, ϕ is the azimuthal angle, $|\uparrow\rangle$ and $|\downarrow\rangle$ are the spin-up and spin-down nucleon spin states.

From Eq. (B6) one can see that a valence nucleon with $m_J=3/2$ can have only spin up, a valence nucleon with $m_J=1/2$ has a 67% probability to have its spin up and a 33% probability to have its spin down, a valence nucleon with $m_J=-1/2$ has a 33% probability to have its spin up and a 67% probability to have its spin down, and a valence nucleon with $m_J=-3/2$ can have only spin down.

Combining this observation with the wave function with $M_J=3/2$, Eq. (5), we obtain the contribution of the three valence nucleons to the cross section

$$\sigma_A^{+,3/2}=\frac{13}{15}\sigma_p^{++}+\frac{2}{15}\sigma_n^{++}+2\sigma_{\rm eff}. \quad \text{(B7)}$$

Here σ_p^{++} (σ_n^{++}) is the $|h\rangle$-proton (nucleon) cross section with parallel spins. In order to obtain Eq. (B7) we used the equality

$$\sigma_p^{++}+\sigma_p^{+-}=2\sigma_{\rm eff},$$
$$\sigma_n^{++}+\sigma_n^{+-}=2\sigma_{\rm eff}. \quad \text{(B8)}$$

Therefore, the total single scattering contribution is

$$\sigma_A^{+,3/2}=\frac{13}{15}\sigma_p^{++}+\frac{2}{15}\sigma_n^{++}+6\sigma_{\rm eff}. \quad \text{(B9)}$$

Note that the last term does not contribute to $\Delta\sigma_A^{\rm Li}$.

Double scattering. Double scattering terms can be of three origins. We can form a pair by coupling six times nonvalence nucleons, by coupling four times a valence and nonvalence nucleons, and by coupling three times valence nucleons.

The contribution of the nonvalence-nonvalence pairs can be computed analytically without numerical integration

$$\sigma_A^{+,3/2}=-\frac{9}{4}\frac{\sigma_{\rm eff}^2}{\pi(R^2+3B)}F(x), \quad \text{(B10)}$$

where $F(x)=\exp(-(q_\parallel R)^2/3)=\exp(-176x^2)$, which originates from the nonvanishing $q_\parallel$. Note that since Eq. (B10) is spin independent, it does not contribute to $\Delta\sigma_A^{\rm Li}$.

The contribution of the valence-nonvalence pairs already requires some numerical integration due to the presence of nontrivial dependence on coordinates of the wave function of the valence nucleons. It is

$$\sigma_A^{+,3/2}=-\frac{\sigma_{\rm eff}}{\pi(R^2+3B)}\left[\frac{13}{15}\alpha_1\sigma_p^{++}+\frac{2}{15}\alpha_1\sigma_n^{++}+\sigma_{\rm eff}\left(\frac{18}{15}\alpha_1+\frac{12}{15}\alpha_3\right)\right]F(x). \quad \text{(B11)}$$

Here $\alpha_1=1.376$ and $\alpha_3=1.795$. Although the x dependence cannot be found in this case in an analytical form, it is very close to $F(x)$. That is why we use the same $F(x)$ for the whole double scattering term.

The contribution of the three valence-valence pairs is quite bulky partially due to the fact that we would like to present it in its natural form, which keeps track of the numerical factors in the wave function (5)

$$\sigma_A^{+,3/2}=-\frac{2\sigma_{\rm eff}}{\pi R^2}\left(\frac{9}{15}\alpha_4\sigma_p^{++}+\frac{4}{15}\alpha_6\sigma_p^{++}+\frac{2}{15}\alpha_6\sigma_n^{++}\right)F(x)-\frac{1}{\pi R^2}\left[\frac{9}{15}\alpha_4\sigma_n^{++}\sigma_n^{+-}+\frac{1}{15}\left(\frac{1}{9}\alpha_4(\sigma_p^{+-}\sigma_n^{++}+\sigma_p^{++}\sigma_n^{+-})\right.\right.$$
$$\left.+\frac{8}{9}\alpha_5(\sigma_p^{++}\sigma_n^{++}+\sigma_p^{+-}\sigma_n^{+-})+\frac{16}{9}\alpha_5(\sigma_p^{++}\sigma_n^{+-}+\sigma_p^{+-}\sigma_n^{++})\right)$$
$$\left.+\frac{4}{15}\left(\frac{1}{9}\alpha_4\sigma_n^{++}\sigma_n^{+-}+\frac{4}{9}\alpha_5(\sigma_n^{++}\sigma_n^{++}+\sigma_n^{+-}\sigma_n^{+-})+\frac{16}{9}\alpha_5\sigma_n^{++}\sigma_n^{+-}\right)\right]F(x). \quad \text{(B12)}$$

Here $\alpha_4=0.300$, $\alpha_5=0.181$, $\alpha_6=0.402$.

Combining all three contributions we find the double-scattering term of the total scattering cross section of the projectile with helicity + off ^{7}Li with $M_J=1/2$

$$\sigma_A^{+,3/2}=-\frac{9}{4}\frac{\sigma_{\rm eff}^2}{\pi(R^2+3B)}F(x)-\frac{\sigma_{\rm eff}}{\pi(R^2+3B)}\left[\frac{13}{15}\alpha_1\sigma_p^{++}+\frac{2}{15}\alpha_1\sigma_n^{++}+\sigma_{\rm eff}\left(\frac{18}{15}\alpha_1+\frac{12}{15}\alpha_3\right)\right]F(x)$$
$$-\frac{2\sigma_{\rm eff}}{\pi R^2}\left(\frac{9}{15}\alpha_4\sigma_p^{++}+\frac{4}{15}\alpha_6\sigma_p^{++}+\frac{2}{15}\alpha_6\sigma_n^{++}\right)F(x)-\frac{1}{\pi R^2}\left[\frac{9}{15}\alpha_4\sigma_n^{++}\sigma_n^{+-}+\frac{1}{15}\left(\frac{1}{9}\alpha_4(\sigma_p^{+-}\sigma_n^{++}+\sigma_p^{++}\sigma_n^{+-})\right.\right.$$
$$\left.+\frac{8}{9}\alpha_5(\sigma_p^{++}\sigma_n^{++}+\sigma_p^{+-}\sigma_n^{+-})+\frac{16}{9}\alpha_5(\sigma_p^{++}\sigma_n^{+-}+\sigma_p^{+-}\sigma_n^{++})\right)+\frac{4}{15}\left(\frac{1}{9}\alpha_4\sigma_n^{++}\sigma_n^{+-}+\frac{4}{9}\alpha_5(\sigma_n^{++}\sigma_n^{++}+\sigma_n^{+-}\sigma_n^{+-})\right.$$
$$\left.\left.+\frac{16}{9}\alpha_5\sigma_n^{++}\sigma_n^{+-}\right)\right]F(x). \tag{B13}$$

In order to find the total scattering cross section on polarized ^{7}Li with $M_J=-3/2$, $\sigma_A^{+,-3/2}$, one should simply switch plus and minus signs in the second place in all the formulas above.

APPENDIX C: SCATTERING OFF POLARIZED ^{7}Li TARGETS WITH $M_J=3/2$ AND $M_J=-3/2$. TRIPLE SCATTERING

The contribution of the triple scattering term to $\Delta\sigma_A^{\rm Li}$ is only 1.6% of the single scattering term and to σ_A is only 0.7% of the single scattering term. To compute its contribution we can combine three nonvalence nucleons, two nonvalence and one valence nucleon, two valence and one nonvalence nucleon, and three valence nucleons. Due to the smallness and complexity of the triple scattering contribution we will give it in a numerical form and only the part of it, which contributes to $\Delta\sigma_A^{\rm Li}$

$$\sigma_A^{+,3/2}=(0.0143\sigma_p^{++}+0.0025\sigma_n^{++}). \tag{C1}$$

Due to cross section fluctuations in the incoming photon, the scattering formalism requires that the triple scattering term should contain $\langle\sigma^3\rangle$, where one averages over fluctuations of the size of the projectile. Our assumption that the incoming photon interacts with the target through the effective state $|h\rangle$ means that we have replaced $\langle\sigma^3\rangle$ by $(\langle\sigma^2\rangle)^2/\langle\sigma\rangle=\sigma_{\rm eff}^2\langle\sigma\rangle$.

In Eq. (C1) $g(x)$ is a function of x slower than $F(x)$, defined $g(0)=1$. In our numerical analysis we set $g(x)=1$ for any x without any loss of accuracy of our results.

In order to find the triple scattering term on polarized ^{7}Li with $M_J=-3/2$, $\sigma_A^{+,-3/2}$, one should simply switch plus and minus signs in the formula above.

APPENDIX D: SCATTERING OFF POLARIZED ^{7}Li TARGETS WITH $M_J=1/2$ AND $M_J=-1/2$.

In this appendix we will give detailed calculations of the total scattering cross section of a polarized incoming hadron with helicity + off a polarized target of ^{7}Li with the z component of the total angular momentum $M_J=1/2$ and $M_J=-1/2$. Following the steps of the Glauber-Gribov formalism described in Appendix B, we will present the single, double, and triple scattering terms.

Single scattering. The total single scattering contribution is a sum of the valence contribution and a simple nonvalence contribution $4\sigma_{\rm eff}$

$$\sigma_A^{+,1/2}=\frac{13}{15}\left(\frac{2}{3}\sigma_p^{++}+\frac{1}{3}\sigma_p^{+-}\right)+\frac{2}{15}\left(\frac{2}{3}\sigma_n^{++}+\frac{1}{3}\sigma_n^{+-}\right)+6\sigma_{\rm eff}. \tag{D1}$$

Double scattering. As in the case of $M_J=3/2$, the double scattering term originates from the three possible ways to form nucleon-nucleon pairs. Similarly to the calculation given in Appendix B we combine all three contributions in order to find the double scattering term of the total scattering cross section of the projectile with helicity + off ^{7}Li with $M_J=1/2$

$$\sigma_A^{+,1/2}=-\frac{9}{4}\frac{\sigma_{\rm eff}^2}{\pi(R^2+3B)}F(x)-\frac{\sigma_{\rm eff}}{\pi(R^2+3B)}\left[\frac{13}{15}\left(\frac{1}{3}\alpha_1\sigma_p^{+-}+\frac{4}{3}\alpha_2\sigma_p^{++}\right)+\frac{2}{15}\left(\frac{1}{3}\alpha_1\sigma_n^{+-}+\frac{4}{3}\alpha_2\sigma_n^{++}\right)\right.$$
$$\left.+\sigma_{\rm eff}\left(\frac{12}{15}\alpha_1+\frac{18}{15}\alpha_3\right)\right]F(x)-\frac{2\sigma_{\rm eff}}{\pi R^2}\left[\frac{9}{15}\left(\frac{1}{9}\alpha_4\sigma_p^{+-}+\frac{8}{9}\alpha_5\sigma_{\rm eff}+\frac{16}{9}\alpha_5\sigma_p^{++}\right)+\frac{4}{15}\left(\frac{1}{3}\alpha_4\sigma_p^{+-}+\frac{4}{3}\alpha_5\sigma_p^{++}\right)\right.$$
$$\left.+\frac{2}{15}\left(\frac{1}{3}\alpha_4\sigma_n^{+-}+\frac{4}{3}\alpha_5\sigma_n^{++}\right)\right]F(x)-\frac{1}{\pi R^2}\left\{\frac{9}{15}\left[\left(\frac{1}{9}\alpha_4+\frac{16}{9}\alpha_5\right)\sigma_n^{++}\sigma_n^{+-}+\frac{4}{9}\alpha_5(\sigma_n^{++}\sigma_n^{++}+\sigma_n^{+-}\sigma_n^{+-})\right]\right.$$
$$\left.+\frac{4}{15}\alpha_4\sigma_n^{++}\sigma_n^{+-}+\frac{1}{15}\alpha_4(\sigma_p^{++}\sigma_n^{+-}+\sigma_p^{+-}\sigma_n^{++})\right\}F(x). \quad \text{(D2)}$$

Here $\alpha_1=1.376$, $\alpha_2=1.002$, $\alpha_3=1.795$, $\alpha_4=0.300$, $\alpha_5=0.181$.

Triple scattering. As it was explained before in Appendix C the triple scattering term is very small. Its 0.8% contribution to the total cross section of the unpolarized $|h\rangle$ off ^{7}Li with $M_J=1/2$ gives a small correction to 11% contribution to shadowing due to the double scattering term. Therefore, we will not give the analytical expression of the triple term but rather will take it into account in numerical results presented in Appendix E.

APPENDIX E: UNPOLARIZED SCATTERING OFF POLARIZED ^{7}Li TARGETS WITH $M_J=3/2$ OR $-3/2$ AND $M_J=1/2$ OR $-1/2$

In this appendix we will present the total scattering cross section of the unpolarized hadronic projectile $|h\rangle$ off a target of ^{7}Li with $M_J=3/2$ and 1/2. We define the cross section off ^{7}Li with $M_J=3/2$ as

$$\sigma_A^{3/2}=\frac{1}{2}(\sigma_A^{+,3/2}+\sigma_A^{-,3/2})=\frac{1}{2}(\sigma_A^{+,3/2}+\sigma_A^{+,-3/2}). \quad \text{(E1)}$$

Using our results of Appendixes B and C and the relation

$$\sigma_p^{++}+\sigma_p^{++}=\sigma_{\rm eff},$$
$$\sigma_n^{++}+\sigma_n^{++}=\sigma_{\rm eff}, \quad \text{(E2)}$$

we obtain for the ratio $\sigma_A^{3/2}/7\sigma_{\rm eff}$, whose deviation from 1 describes nuclear shadowing,

$$\frac{\sigma_A^{3/2}}{7\sigma_{\rm eff}}=1-\frac{9}{28}\frac{\sigma_{\rm eff}}{\pi(R^2+3B)}F(x)-\frac{\sigma_{\rm eff}}{\pi(R^2+3B)}\times\left(\frac{33}{15}\alpha_1+\frac{12}{15}\alpha_3\right)\frac{1}{7}F(x)-\frac{\sigma_{\rm eff}}{\pi R^2}\left(\frac{28.3}{15}\alpha_4+\frac{32}{15}\alpha_5+\frac{12}{15}\alpha_6\right)\frac{1}{7}F(x)+0.0061g(x). \quad \text{(E3)}$$

The last term is the triple scattering term. After having substituted all numerical factors we obtain

$$\frac{\sigma_A^{3/2}}{7\sigma_{\rm eff}}=1-0.0922e^{-176x^2}+0.0061g(x). \quad \text{(E4)}$$

The scattering cross section of the unpolarized $|h\rangle$ off the ^{7}Li target with $M_J=-3/2$ is the same.

Similarly to the above calculations and using Appendix D, we can present the ratio $\sigma_A^{1/2}/7\sigma_{\rm eff}$ for the target with $M_J=1/2$

$$\frac{\sigma_A^{1/2}}{7\sigma_{\rm eff}}=1-\frac{9}{28}\frac{\sigma_{\rm eff}}{\pi(R^2+3B)}F(x)-\frac{\sigma_{\rm eff}}{\pi(R^2+3B)}\times\left(\frac{12}{15}\alpha_1+\frac{33}{15}\alpha_3\right)\frac{1}{7}F(x)-\frac{\sigma_{\rm eff}}{\pi R^2}\left(\frac{9}{15}\alpha_4+\frac{72}{15}\alpha_5+\frac{12}{15}\alpha_6\right)\frac{1}{7}F(x)+0.0083g(x). \quad \text{(E5)}$$

Numerically, this ratio is

$$\frac{\sigma_A^{1/2}}{7\sigma_{\rm eff}}=1-0.1069e^{-176x^2}+0.0083g(x). \quad \text{(E6)}$$

We used Eqs. (E4) and (E6) to find the scattering cross section of the unpolarized projectile off an unpolarized ^{7}Li target.

[1] V.N. Gribov, Yad. Fiz. **9**, 640 (1969) [Sov. J. Nucl. Phys. **9**, 369 (1969)]; Zh. Éksp. Teor. Fiz. **56**, 892 (1969) [Sov. Phys. JETP **29**, 483 (1969)]; **57**, 1306 (1969) [**30**, 709 (1970)].

[2] L. Alvero, L. L. Frankfurt, and M. Strikman, Eur. Phys. J. A **5**, 97 (1999); L. L. Frankfurt and M. Strikman, *ibid.* **5**, 293 (1999).

[3] L. Frankfurt and M. Strikman, Phys. Rep. **160**, 235 (1988).

[4] L. Frankfurt, M. Strikman, and S. Liuti, Phys. Rev. Lett. **65**,

1725 (1990).
[5] T. Gousset and H.J. Pirner, Phys. Lett. B **375**, 349 (1996).
[6] D.M. Alde *et al.*, Phys. Rev. Lett. **64**, 2479 (1990).
[7] C. Ciofi degli Atti, E. Pace, and G. Salme, Phys. Rev. C **46**, R1591 (1992); R.-W. Schulze and P.U. Sauer, *ibid.* **48**, 38 (1993); R.-W. Schulze and P.U. Sauer, *ibid.* **56**, 2293 (1997).
[8] C. Ciofi degli Atti, E. Pace, and G. Salme, Phys. Rev. C **48**, R968 (1993); L. Kaptari and A. Umnikov, Phys. Lett. B **240**, 203 (1990).
[9] L. Frankfurt, V. Guzey, and M. Strikman, Phys. Lett. B **381**, 379 (1996).
[10] J. Edelmann, G. Piller, and W. Weise, Z. Phys. A **357**, 129 (1997); Phys. Rev. C **57**, 3392 (1998).
[11] D. Crabb (private communication).
[12] L.D. Landau and E.M. Lifshitz, *Quantum Mechanics, Non-relativistic Theory* (Pergamon, New York, 1977).
[13] G. Altarelli, R. Ball, S. Forte, and G. Ridolfi, hep-ph/9803237.
[14] T.H. Bauer, R.D. Spital, D.R. Yennie, and F.M. Pipkin, Rev. Mod. Phys. **50**, 260 (1978); **51**, 407(E) (1979).
[15] R.L. Jaffe and A. Manohar, Nucl. Phys. **B321**, 343 (1989).
[16] B. Adeva *et al.*, preprint CERN-EP/98-85.
[17] C.D. Goodman and S.D. Bloom, in *Spin Excitations in Nuclei*, edited by F. Petrovich *et al.* (Plenum, New York, 1984), p. 143.
[18] J.F. Germound and C. Wilkin, Phys. Lett. **59B**, 317 (1975).
[19] M. Strikman, *Proceedings of the Symposium on Spin Structure of the Nucleon*, Yale, 1994, edited by V.H. Hughes and C. Cavata (World Scientific, Singapore, 1995).
[20] N.N. Nikolaev and W. Schäfer, Phys. Lett. B **398**, 254 (1997).
[21] L. Alvero, J.C. Collins, and J.J. Whitmore, hep-ph/9806340; L. Alvero, J.C. Collins, and J.J. Whitmore, Phys. Rev. D **59**, 074022 (1999).